LRP 589/97 October 1997

ON RESONANCE ABSORPTION AND CONTINUUM DAMPING

A. Jaun, K. Appert, T. Hellsten,
J. Vaclavik, L. Villard

submitted for publication to
Phys. Rev. Lett.

Annex:

Prediction of Alfvén eigenmode dampings in the
Joint European Torus
A. Jaun, A. Fasoli, W.W. Heidbrink
submitted for publication to Phys. Rev. Lett.

On Resonance Absorption and Continuum Damping

A. Jaun[1,2], K. Appert[1], T. Hellsten[2], J. Vaclavik[1], L. Villard[1]

[1] CRPP-EPFL, CH-1015 Lausanne, Switzerland

[2] Alfvén Laboratory, EURATOM-NFR Association, KTH, SE-100 44 Stockholm, Sweden

ABSTRACT. The absorption of power is studied with fluid and gyrokinetic plasma models, when two Alfvén or ion-ion hybrid resonances provide for a weak damping in a partially standing wavefield. Examples chosen in slab and toroidal geometry show that the the fluid predictions based on resonance absorption are generally very different from the Landau damping of mode-converted slow waves. They in particular suggest that the continuum damping of toroidal Alfvén eigenmodes (TAE) and the power deposition profiles obtained in the ion-cyclotron range of frequencies (ICRF) using fluid plasma models are very misleading.

PACS numbers: 52.35.Bj, 52.35.Py, 52.50.Gj, 52.65.Tt

Ever since Landau's lesson, which lead to the discovery of the damping associated with the wave-particles resonance, it has been recognized that the integration over time of partial differential equation singularities requires a careful treatment that guarantees in effect that the causality remains preserved. By analogy, when the fluid wave equations are integrated in presence of an Alfvén or ion-ion hybrid resonance, a residual absorption of power appears which may be evaluated either by taking into account an arbitrarily small dissipation of the plasma or by adding artificially an imaginary part to the frequency. Studying the propagation of the fast-magnetosonic wave in the ion-cyclotron range of frequencies (ICRF), Budden [1] for example determined the fraction of the power absorbed, transmitted and reflected by a resonance-cutoff pair using a fluid plasma model, without specifying the mechanism actually responsible for the power dissipation.

If the plasma temperature is sufficiently large, the resonant layers where the fluid equations are singular coincide with the location where the fast wave energy can be converted to slow kinetic waves owing their existence to the finite Larmor radius (FLR) excursion of the ions [2]. The change of polarization accompanied with a rise in the electric field component parallel to the magnetic field is then generally responsible for the power dissipation, with resonant wave-particle interactions that occur as the slow wave propagates away from the conversion layer. Using an FLR expansion [3, 4, 5] and solving the full non-local problem [6], it has been found that the total power converted from a fast wave traveling in a single pass through a resonance depends only weakly on the slow wave parameters; the resonance absorption from fluid plasma models then coincides to a good degree of accuracy with the Landau damping of the slow wave described by the gyrokinetic models.

The aim of this letter is to draw attention to the fact that this is not in general true when two resonances are present in the same global wavefield, this even when the slow wave is damped in the vicinity of the mode conversion surface. In particular, the continuum damping of Alfvén eigenmodes (AE) [7, 8] and the resonance absorption of ICRF driven wavefields calculated with toroidal fluid plasma models [9, 10] are shown to be dramatically different from our gyrokinetic calculations, suggesting that AE mode stability threshold and ICRF power deposition profile predictions are very questionable when using fluid models.

To illustrate the concept first in a simple shearless slab plasma, Fig.1 shows an Alfvén wave heating scenario similar to the TCA tokamak [11] (B_0=1.5 T, $n_{e,0} = 2.3 \times 10^{19}$ m^{-3}, $T_{D,0}$=350 eV, $f_{ant} = 2$ MHz, $k_y = -5$ m^{-1}, $k_z = 2.9$ m^{-1}). An antenna current is imposed in the vacuum region on the right ($x = x_a = +19$ cm) and launches an evanescent fast wave into the plasma ($|x| < x_p = 18$ cm). After reflections, a global wavefield is created oscillating in phase in the entire cavity bounded by perfectly conducting walls ($|x| = x_w = 21$ cm). A parabolic variation of the density $n_e(x) = n_D(x) = n_{e,0}[1 - 0.95(x/x_p)^2]$ generates two Alfvén resonances at $|x| = x_r = 9.2$ cm, which are set to electron temperatures that differ

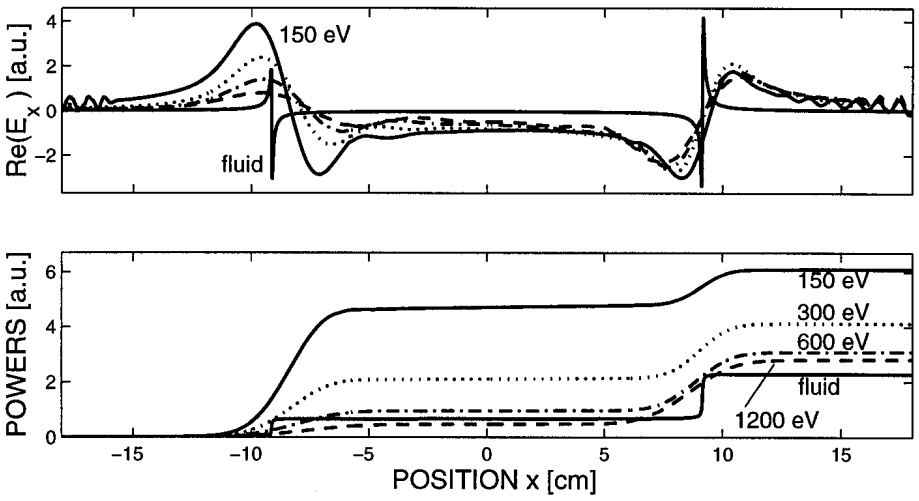

Figure 1: Alfvén wave heating scenario in a TCA-like slab plasma driven with an antenna from the right. The wavefield $Re(E_x)$ (top) and the integrated power $P(x)$ (bottom) calculated using a fluid model are compared with their gyrokinetic counterparts obtained for a rising temperature $T_{e,0}$ = 150, 300, 600, 1200 eV. The conversion layers are set to temperatures that differ by more than a factor two with an asymmetric profile of the form $T_e(x) = T_{e,0}[1 - 0.95(x/18)^2]^2[1 - 0.5(x/18)]^2$.

by more than a factor two $T_e(x) = T_{e,0}[1 - 0.95(x/x_p)^2]^2[1 - 0.5(x/x_p)]^2$, keeping that of the deuterons equal on both sides $T_D(x) = T_{D,0}[1 - 0.95(x/x_p)^2]^2$ eV. Using the full wave code ISMENE [12, 13] to compute the perpendicular wavefield (E_x, E_y) with a cold-fluid plasma model (see Ref.[13], eqs.6.1-6.2), sharp variations appear at the resonances which have been numerically resolved in Fig.1(top) by adding a small imaginary part $\delta = 0.02$ to the antenna frequency $\omega = 2\pi f_{ant}(1 + i\delta)$. Apart from details in the vicinity of the resonant layers, a change of the artificial damping $\delta \in [0.002; 0.02]$ does neither affect the integrated power $P(x) = \int_{-x_p}^{x} Im[\frac{\omega}{8\pi} Im(\mathbf{E}^* \cdot \epsilon \cdot \mathbf{E})]dx'$ in Fig.1(bottom) nor does it modify the relative power fraction absorbed at each resonance (table 1, fluid), suggesting that the power resonantly absorbed does not depend on the manner how the equations are regularized.

This fluid calculation has now to be contrasted with the gyrokinetic results from the same code, when all the wavefield components (E_x, E_y, E_z) are solved in terms of a second order FLR expansion of the plasma dielectric tensor (see Ref.[13], eqs.6.17-6.20). Fig.1(top) shows that a mode-converted kinetic Alfvén wave (KAW) propagates inwards from both sides and gets immediately damped by Landau interactions with the electrons in the neighborhood of the conversion layer. The short wavelength oscillations in the edge region ($|x| > 12$ cm) come from the surface quasi-electrostatic wave (SQEW) which is directly excited at the plasma boundary, but is unimportant for the subsequent analysis. Rising the electron temperature in the center $T_{e,0} = 150, 300, 600, 1200$ eV while keeping that of the ions fixed, Fig.1(bottom) shows that the integrated power profile $P(x)$ is changing: not only the total power absorption is mod-

$T_{e,0}$ [eV]	$f^{left}_{x=-x_r}$ [%]	$f^{right}_{x=+x_r}$ [%]
150	78	22
300	51	49
600	44	56
1200	17	83
fluid model	30	70

Table 1: Fraction of the power absorbed by each resonance, based on the fluid and gyrokinetic power deposition profiles in Fig.1(bottom)

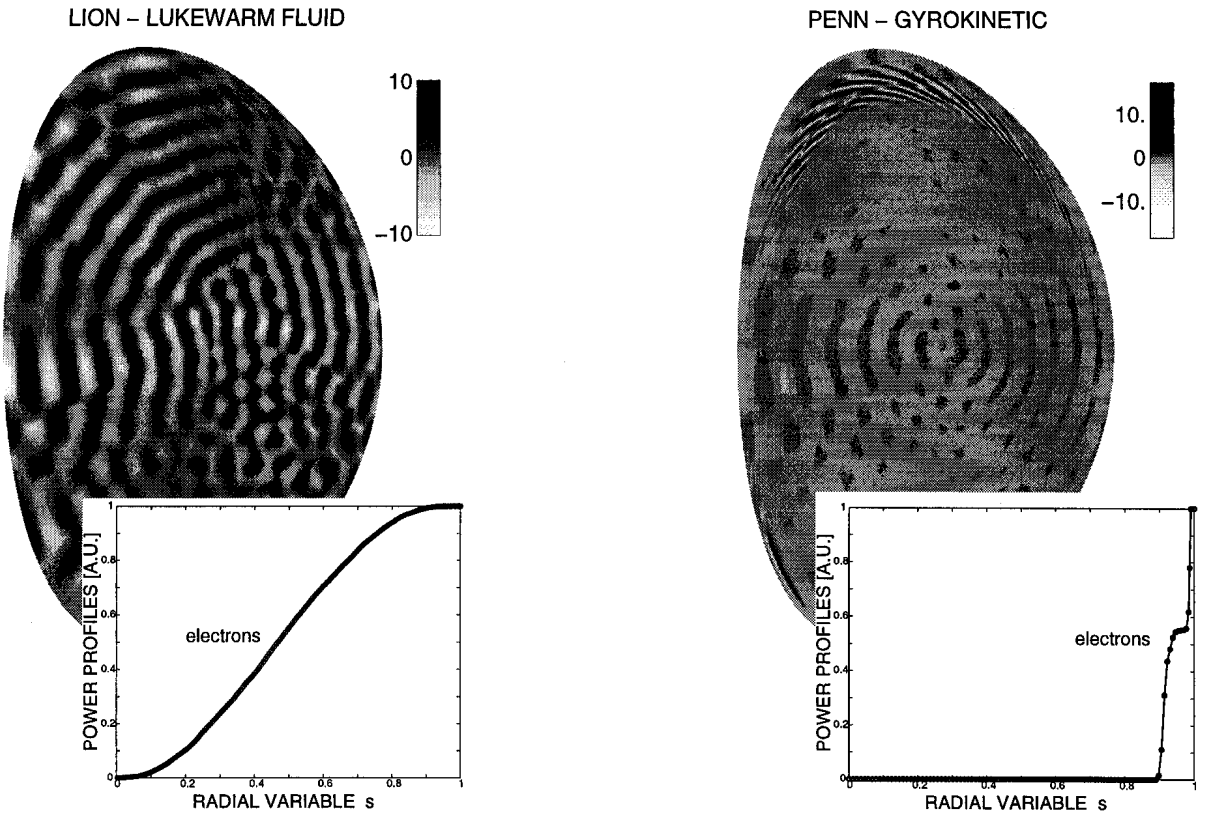

Figure 2: Current drive scenario proposed in Ref.[16] for ITER. The global wavefield $Re(E_n)$ (top) and the integrated power profile $P(s)$ (bottom) both show that the mode-conversion predicted by the gyrokinetic PENN calculation (right) is not reproduced with resonance absorption in the fluid LION code (left), suggesting that fluid predictions can be very misleading.

ified, but also the fraction absorbed by each resonance is dramatically different (table 1). This strong dependence on the temperature is of course not reproduced with the fluid plasma model and is in apparent contradiction with the small dependence on the slow wave parameters which has previously been observed in other comparisons. The paradox is solved by realizing that a small change in the "single pass" mode-conversion efficiency, which is rendered visible because of the temperature asymmetry, is here strongly amplified when the global wavefield carries fast wave energy from one resonance to the other.

This phenomenon, which has for simplicity been illustrated with the simple slab calculation above, becomes particularly important in tokamaks and stellarators where the magnetic curvature and the finite frequency in the ion-cyclotron range couple different poloidal and toroidal harmonics, forming global modes which can interact with resonant surfaces throughout the plasma radius. Alfvén eigenmodes get damped by resonances, but the continuum damping predicted using fluid plasma models [7, 8] sometimes disagrees by an order of magnitude with the gyrokinetic predictions and the experimental measurements [14, 15]. ICRF heating scenarii generally involve a multitude of resonances with large poloidal mode numbers $|m| > 20$. Global fluid calculations suggest that they are generally not excited because the geometrical coupling, proportional to the inverse aspect ratio power $\epsilon^{|m-m_{ant}|}$, is very weak for low antenna mode numbers $|m_{ant}| \sim 5$. The gyrokinetic calculations from Ref.[16] however show that large poloidal mode numbers appear because of the toroidicity, when the fast and KAW wavelengths match at a resonance $\vec{k}_{fast} = \vec{k}_{slow}$ where the thermal electron velocity exceeds the parallel wave phase velocity $\omega/(k_{\|} v_{th,e}) < 1$.

The second example illustrates this in Fig.2 with a current-drive scenario proposed in Ref.[17] for the international thermonuclear experimental reactor (ITER) (B_0=6 T, $q_0 = 1.03$, $\beta_{tor} = 2.7\%$, $n_{e,0} = 1.4 n_{D,0} = 3.5 n_{T,0} = 1.4 \times 10^{20}$ m^{-3}, $T_{e,0} = T_{D,0} = T_{T,0} = 19$ keV, $f_{ant} = 20$ MHz, $n_{tor} = 21$). The lukewarm fluid LION code [9] calculation in Fig.2(left) suggests that the fast wave emmitted by

an antenna on the low magnetic field side of the torus, first propagates inwards past the magnetic axis and forms a partially standing global wavefield that extends throughout the torus. The coupling to high poloidal mode numbers is however sufficiently weak that the resonance absorption remains negligible and the power gets almost homogeneously absorbed by the fast wave electron Landau damping and transit-time magnetic pumping (TTMP). This fluid prediction is dramatically different from the gyrokinetic result obtained from the PENN code [16], which shows that strong mode-conversion takes place where the partially standing fast wavefield meets the KAW scalelength in the neighbourhood of fluid resonances with large poloidal mode numbers $m \simeq 25$. The power is then mainly deposited by the electron Landau damping of the KAW, in the plasma edge region where the resonance absorption computed with fluid plasma models remains negligible. Apart form questioning the validity of fluid plasma models for weak absorption, this mode-conversion at the plasma edge provides for a plausible mechanism explaning the degradation in the heating efficiency which has been observed in the experiments [18].

In summary, both examples chosen above in slab and toroidal geometry show that fluid plasma models cannot be used to correctly predict the power absorption and the continuum damping when two resonances or more are present in a partially standing wavefield. This is in particular true for the prediction of Alfvén eigenmode dampings and the modeling of the power deposition profiles during ICRH, where more sophisticated gyrokinetic descriptions are required - at least.

One of the authors (A.J.) acknowledges useful discussions with F. Zonca. This work was supported in part by the Swiss and the Swedish National Science Foundations and the calculations were performed on the CRAY C-94 super-computer in Linköping.

References

[1] K. Budden, *Radio Waves in the Ionosphere*, Cambridge University Press (1985) 596

[2] A. Hasegawa, L. Chen, Phys. Rev. Lett. **35** (1975) 370

[3] D.G. Swanson, Phys. Fluids **24** (1981) 2035

[4] P. Colestock, R. Kashuba, Nucl. Fusion **23** (1983) 763

[5] J.A. Heikkinen, T. Hellsten, M.J. Alva, Nucl. Fusion **31** (1991) 417

[6] O. Sauter, J. Vaclavik, Comput. Phys. Commun **84** (1994) 226

[7] M. N. Rosenbluth, H.L. Berk, J.W. Van Dam, D.M. Linberg, Phys. Rev. Lett. **68** (1992) 596

[8] F. Zonca, L. Chen, Phys. Rev. Lett. **68** (1992) 592

[9] L. Villard, K.Appert, R.Gruber, J.Vaclavik, Comput.Phys.Reports **4** (1986) 95

[10] D. Gambier, A. Samain, Nucl. Fusion **25** (1985) 283

[11] G.A.Collins, F.Hofmann, B.Joye, Phys. Fluids **29** (1986) 2260

[12] K.Appert, T.Hellsten, J.Vaclavik, L.Villard, Comput. Phys. Commun. **40** (1986) 73

[13] J. Vaclavik, K. Appert, Nucl. Fusion **31** (1991) 1945

[14] A. Jaun, A. Fasoli, W.W. Heidbrink, Phys. Rev. Lett., submitted

[15] A. Fasoli, J. Lister, J.-M. Moret, S. Sharapov, D. Borba, G. Bosia, D. Campbell, J. Dobbing, C. Gormezano, J. Jacquinot, P. Lavanchy, Ph. Marnillod, A. Santagiustina, Phys. Rev. Lett. **75** (1995) 645

[16] A. Jaun, K. Appert, J. Vaclavik, L. Villard, Comput. Phys. Commun. **92** (1995) 153

[17] *Fast Wave Heating and Current Drive in ITER*, Eur. Coord. Comm. on Fast Wave Current Drive and Heating (CCFW), edited by V. Bhatnagar, J. Jacquinot, NET Report EUR-FU/XII/163/94 (1994)

[18] L.-G. Eriksson, T. Hellsten, Nucl. Fusion **29** (1989) 875

ANNEX

(submitted to Phys. Rev. Lett.)

Prediction of Alfvén Eigenmode Dampings in the Joint European Torus

A. Jaun[1], A. Fasoli[2,3], W. W. Heidbrink[4]

[1] Alfvén Laboratory, EURATOM-NFR Association, KTH, SE-100 44 Stockholm, Sweden
[2] CRPP-EPFL, CH-1015 Lausanne, Switzerland
[3] JET Joint Undertaking, Abingdon, Oxon, OX14 3EA, UK
[4] University of California, Irvine, CA, USA

ABSTRACT. Predictions from a gyrokinetic toroidal plasma model reproduce for the first time the evolution of Alfvén eigenmode dampings measured in JET over a range of discharges, providing for a credible capability to predict the stability of perturbations which are known to be near to marginal in the International Thermonuclear Experimental Reactor (ITER). The coupling between global shear- and kinetic-Alfvén waves is responsible for the main source of damping through resonant interactions and can be an order of magnitude larger than the fluid predictions which neglect global kinetic effects.
PACS numbers: 52.55.Fa, 52.35.Py, 52.40.Fd, 52.65.Tt

Whether global modes of the Alfvén wave driven by fusion-born $\alpha-$particles are stable is a critical issue for fusion devices such as the International Thermonuclear Experimental Reactor (ITER). The growth rate of the instability depends on the strength of the $\alpha-$particle pressure gradient drive, which has to remain smaller than the overall damping from the collisions and the resonant Landau interactions between the particles and the wavefield. Because the predictions are very sensitive to the spatial structure of the eigenmode which in turn depends on the equilibrium profiles, magnetohydrodynamic (MHD) stability codes have been developed modeling the bulk plasma with an ideal or resistive fluid [1, 2, 3, 4]. Growth rates may be evaluated approximatively from the shear-Alfvén wavefield with simplified models including direct Landau damping [5, 4], continuum damping [6, 7], and radiative damping [8]. Even if the theoretical calculations [4, 9] performed in this manner could only occasionally explain the observed instability thresholds when the mode coupling to kinetic waves did not affect the eigenmode structure, it is remarkable how the theoretical understanding of the beam Landau damping [10] paved the way to the first observation of $\alpha-$particle driven toroidicity Alfvén eigenmodes (TAE) [11].

A proper evaluation of the growth rate requires taking into account the finite ion gyro-radius responsible for the mode conversion from fast to slow waves such as the kinetic-Alfvén [12] and the drift waves. This generally occurs when the spatial scale of two waves match at a resonance, but can also be induced through mode coupling by the magnetic field curvature [13, 14] and, as will be shown below, by the weak magnetic shear in the plasma core. In this letter, the gyrokinetic predictions are found to agree with the measured frequencies and damping rates [15] over a range of discharges and times, this in contrast with computed damping rates that are an order of magnitude smaller when global kinetic effects are neglected; apart from quantifying for the first time the relative importance of what could be associated in simplified models with continuum and radiative damping, the results illustrate that when the central magnetic shear $\hat{s} = \frac{\rho}{q}\frac{\partial q}{\partial \rho}$ is smaller than

$\epsilon = \frac{\rho}{R}$ the inverse aspect ratio, there can be a dramatic change in the AE structure due to mode conversion to the kinetic-Alfvén wave, which strongly enhances the Landau absorption in the plasma core. The calculations also show the stabilizing effect of a high magnetic shear at the plasma edge, giving a plausible explanation why antenna excited AE have never been observed in JET X-point configurations. To our knowledge, this study is the most detailed comparison which has been undertaken between a non-ideal MHD spectrum and experimental measurements; it also provides a strong validity check for the ITER predictions, showing that in a reference equilibrium, Alfvén eigenmodes (AE) with low to intermediate toroidal mode numbers $n = 1 - 12$ are stable for a large variety of burn conditions [16].

Having chosen a discharge with good damping measurements, the equilibrium magnetic field, the density and temperature profiles have been reconstructed with the best possible fit to the experimental diagnostics [17, 18]. The gyrokinetic toroidal PENN code [19] is then used to predict the spectrum from the equilibrium data only, monitoring the response peaks in the same manner as in the experiment [15] to determine the frequency and damping of AEs that are sufficiently global to reach the saddle coil antenna at the bottom of the plasma. The plasma model [20] is based on a finite Larmor radius expansion for the passing bulk particles and takes into account the drifts induced by the equilibrium inhomogeneities. Resonant wave-particle interactions are modeled with an approximate functional dependence for the parallel wave vector $k_{\|} = n/R$, where n is the toroidal mode number and R the major radius. The PENN code has been successfully tested for heating scenarios from the ion-Bernstein [21] down to the Alfvén range of frequencies [19], and has been validated for lower frequencies with measurements of the AE spectrum [22] and eigenmode structures [23] in the JET tokamak.

The first discharge being analyzed (No.31561 at 10 sec) is an ohmic fat pear-shaped plasma with a weak magnetic shear $\hat{s} < \epsilon$ from the core out to a normalized radius $s = \sqrt{\psi} \simeq 0.18$, where ψ stands for the poloidal magnetic flux. The safety factor $q(s)$ rises rapidly towards the edge so that a multitude of gaps appears in Fig.1(a) by the coupling of neighboring poloidal Fourier harmonics $m = -2, ... - 10$. The mis-alignment of individual gap frequencies (which decrease as $1/q\sqrt{n_D}$ when moving radially outward) formally closes the global gap in the fluid spectrum, so that an Alfvén resonance remains in the plasma for all frequencies. Scanning the interval [120; 180] kHz, an AE is predicted at 161 kHz with a damping rate of $\gamma/\omega_{pred} = 0.013 \pm 0.003$, where the uncertainty refers to oscillations in the numerical convergence. A single eigenmode is also observed in the experiment with a frequency of 131 kHz which is somewhat lower, probably because of the uncertainty in the core on the safety factor which is larger when no sawtooth inversion radius can be used as a diagnostic; the damping rate $\gamma/\omega_{exp} = 0.0146$ is however in very good agreement with the predicted value. Fig.1(b) shows that the mode has a global radial extension; the toroidicity induced variation of the shear-Alfvén wavefield matches the kinetic-Alfvén wavelength in the $(-2, -3)$ TAE gap and creates a standing wave between the mode cou-

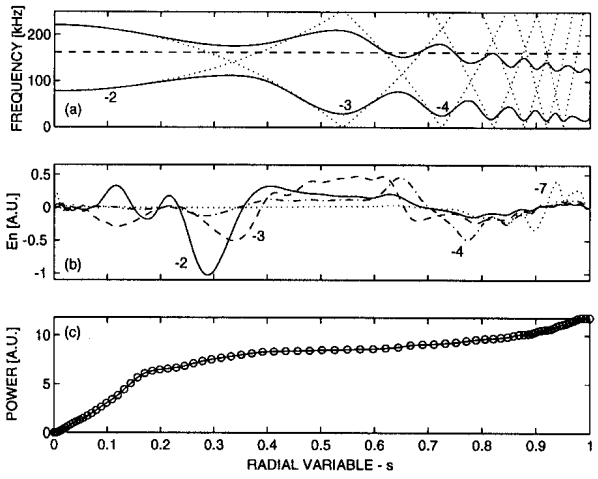

Figure 1: TAE mode $n = 2$ at 161 kHz in the discharge No.31561 at 10 sec with parameters $B_T = 1.65$ T, $q_0 = 1.13$, $q_a = 5.49$, $n_e(0) = n_D(0) = 1.6 \times 10^{19} m^{-3}$, $T_e(0) = T_D(0) = 2$ keV. The plots show a sketch of the Alfvén gap structure with a dashed line for the global AE frequency (a), the Fourier components of the radial electric field $\Re e(E_n)$ in (b) and $P(s)$ the power absorption integrated from the center (c), with circles identifying the radial discretization as a function of the normalized radius s.

pling region around $s = 0.35$ and the plasma core [13]. The electric field component parallel to the magnetic field $E_{||}$ gives rise to an electron Landau damping which can be partitioned with the integrated power $P(s) = \int_0^s P(s')ds'$ in Fig.1(c) into: 70% absorbed by the kinetic-Alfvén wave induced in the core where no resonance is present, 5-10% by mode conversion at Alfvén resonances ($s = 0.62, 0.68, 0.75$), and a remaining 20-25% by direct Landau damping of the shear-Alfvén wavefield in the edge region, where the enhanced magnetic shear localizes the mode radially and thereby increases the absorption. From the wavefield, it is clear that simplified models such as radiative damping and continuum damping are not applicable, the first because a standing kinetic wave is created in the core and the second because the kinetic wavelength is comparable with the gap size.

The second discharge (No.33273 at 16.35 sec) is an elongated pear-shaped plasma which has been examined experimentally in Ref.[23]. Two global AE are predicted in the interval [100; 300] kHz, one around 140 kHz with a weak antenna coupling and relatively large damping and a second with a 30 times better coupling at 266 kHz and a weak damping $\gamma/\omega_{th}^{EAE} = 0.0026 \pm 0.0004$ which depends rather sensitively on the magnetic shear. Two modes are also found in the experiment at 142 kHz and 277 kHz; the first disappears in the sweep 1 sec later, in agreement with the theoretical prediction of weak coupling for the lower frequency mode , while the damping measured for the second $\gamma/\omega_{exp}^{EAE} = 0.0014$ is a factor two smaller than the experimental value . Fig.2 shows that 60% of the electron Landau absorption occurs through mode conversion at the Alfvén resonances ($s = 0.52, 0.83$), another 20% by mode coupling in the weak magnetic shear region ($s < 0.17$) and a remaining 20% by direct damping of the shear-Alfvén wavefield in the edge where the magnetic shear is stronger. Further studies carried out by varying the equilibrium parameters again [13, 22] show that when the damping is as small as $\gamma/\omega \simeq 0.001$, the theoretical result depends rather sensitively on the equilibrium profiles, and that a $\sim 5\%$ uncertainty in the safety factor can account for the factor two discrepancy in the damping.

A third series of predictions has been carried out for the discharge No.38573 in which the evolution of an AE has been measured from its birth around

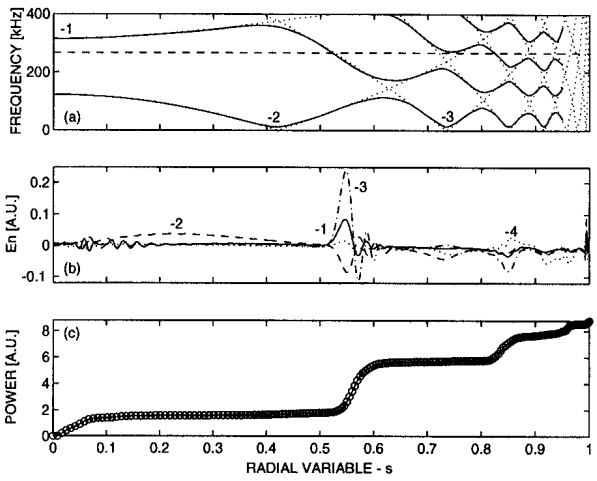

Figure 2: $n = 2$ EAE mode at 266 kHz in the discharge No.33273 at 16.35 sec with parameters $B_T = 3.1$ T, $q_0 = 0.86$, $q_a = 4.46$, $n_e(0) = n_D(0) = 4.48 \times 10^{19} m^{-3}$, $T_e(0) = T_D(0) = 2$ keV. Same type of plots as in Figure 1.

3 sec when a $(-1, -2)$ TAE gap is formed around $q_0 = 1.5$ on the plasma axis, drifting first rapidly outward to $s \simeq 0.55$ at 4.7 sec, with the AE going through a non-resonant 80 keV beam heating phase between 5.5-7.5 sec, until it again disappears after 10 sec when an X-point is formed at the bottom of the elliptical plasma and the safety factor in the core finally reaches a minimum of $q_0 = 0.92$. Two global kinetic Alfvén eigenmodes (KAE) [13, 22] are predicted in the interval [160; 210] kHz, with wavefields that reflect the $l = 0, 1$ radial oscillations of the kinetic-Alfvén wave modulating the TAE wavefield inside the $(-1, -2)$ gap.

Because the interval scanned experimentally is very small $\Delta\omega \simeq 3\gamma_{exp}$ and the antenna coupling to the higher frequency $l = 0$ mode predicted to be better until 4.7 sec, only the high frequency KAE appears on the measurements. Fig.3 shows that the predicted AE frequencies fall within $\sim 3\%$ of the experimental measurements, reproducing well the strong variation from the beam fueling. The agreement achieved for the damping is around 30% for most of the discharge except in the beginning when the gap position varies very rapidly, making the predictions very sensitive to the mode conversion parameters in the plasma core. This is clearly ap-

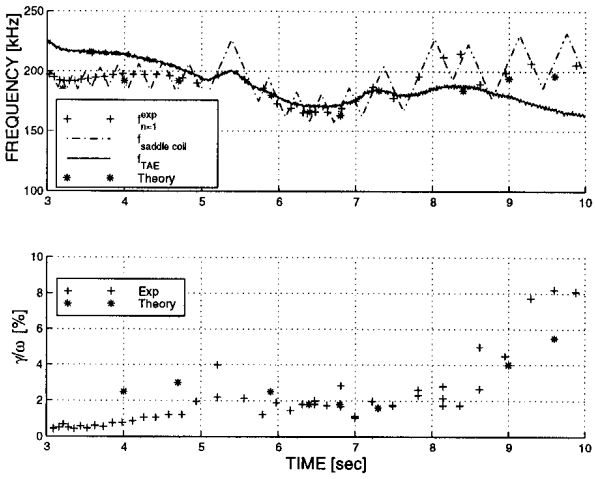

Figure 3: Comparison between the AE frequencies (top) and dampings (bottom) *predicted* (*) and measured (+) during the evolution in the discharge No.38573. Experimentally, the systematic error from the choice of the relevant diagnostic channels to fit is the dominant source of uncertainty ($\sim 10-30\%$ for γ/ω); for the theory the uncertainty comes mainly from the reconstruction of the safety factor profile ($\sim 10-20\%$ for q_0). Parameters at 4.0 sec are $B_T = 2.56$ T, $q_0 = 1.36$, $q_a = 4.62$, $n_e(0) = n_D(0) = 1.75 \times 10^{19} m^{-3}$, $T_e(0) = 2.62$ keV, $T_D(0) = 1.97$ keV.

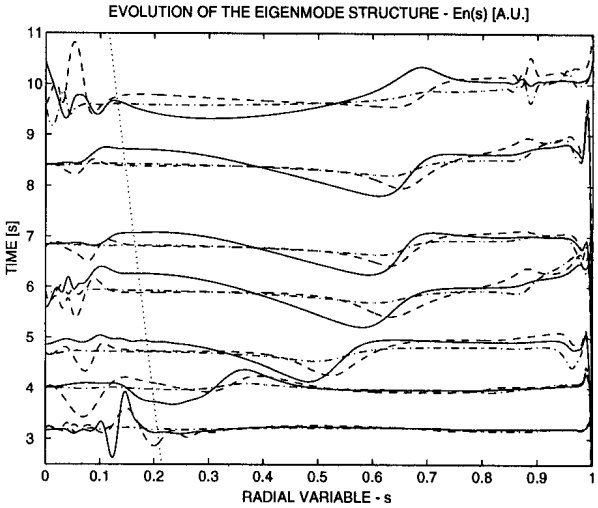

Figure 4: Evolution of the theoretical eigenmode structure $\Re e(E_n)$ in the discharge No.38573. The dotted line locates the weak shear region in the core where $\hat{s} = \epsilon$.

parent in the wavefields of Fig.4, where the kinetic-Alfvén wave dominates the mode structure until 4.7 sec. Most important however is that the largest fraction of the Landau damping from 4.0 to 8.4 sec is here induced by short wavelength oscillations in the plasma core: removing the kinetic effects artificially from the model for small radii ($s < 0.2$) yields electron Landau damping rates from mainly the shear Alfvén wave of $\gamma/\omega_{art} \simeq 0.003$, an order of magnitude smaller than observed in the experiment. Since the gap opens up monotonically from $s \simeq 0.65$ to the center, this core-localized mode conversion has to be of different nature than the mode coupling induced inside the toroidicity gap [13]. Studies carried out by varying locally the central magnetic shear show that the oscillations are caused by an increase of the kinetic-Alfvén wavelength in the weak shear region, resulting in a mode conversion once the spatial scale of the kinetic-Alfvén wave matches the shear-Alfvén wavefield scale length. Because of the complicated nature of this mechanism, we believe that it is not possible to derive a simplified model that fits well the global AE measurements. Instead, we use here the predictions from the comprehensive PENN model to illustrate the phenomenon and show not only that it is important, but that it is also in agreement with the measurements. Another important effect apparent in figures 3 and 4 which becomes dominant after ~ 8 sec, is the enhanced global damping rate due to the radial localization of the shear-Alfvén wavefield in the edge region. This is caused by the rise of the edge magnetic shear associated with the formation of the X-point and explains why antenna excited AE have never been observed in JET in the presence of X-points.

In summary, gyrokinetic calculations of global AE dampings predicted for JET plasmas are in good agreement with the measurements and the uncertainties obtained show to which extent predictions are possible for ITER. Resonant Landau interaction with the global shear- and kinetic-Alfvén wavefield provide for the dominant damping mechanism, with mode conversion induced by Alfvén resonances, toroidal mode coupling and the weak magnetic shear in the plasma core.

Help from D. Borba, O. Sauter for the equilibrium reconstruction, P. Lavanchy for the experimental support and useful discussions with T. Hellsten, J. Vaclavik, L. Villard are gratefully acknowledged. This work was supported in part by the Swedish (A.J.), the Swiss (A.F.) National Science Foundations, and the subcontract SC-L134501 to the U.S. DOE contract DE-AC03-89ER51114 (W.W.H.). The experiments have been carried out within a JET/CRPP task agreement and the calculations performed on the CRAY C-94 supercomputer in Linköping and the NEC SX-4 in Manno.

References

[1] C. Z. Cheng, Phys.Reports **211** (1992) 1

[2] A. D. Turnbull *et al.*, Phys.Fluids B **5** (1993) 2546

[3] G. T. Huysmans, J. P. Goedbloed, W. Kerner, Phys. Fluids B **5** (1993) 1545

[4] L. Villard, S. Brunner, J. Vaclavik, Nucl. Fusion **35** (1995) 1173

[5] R. Betti, J. Freidberg, Phys. Fluids B **4** (1992) 1465

[6] M. N. Rosenbluth *et al.*, Phys. Rev. Lett. **68** (1992) 596

[7] F. Zonca, L. Chen, Phys. Rev. Lett. **68** (1992) 592

[8] R. R. Mett, E. J. Strait, S. M. Mahajan, Phys. Plasmas **1** (1994) 3277

[9] G. Y. Fu, C. Z. Cheng, K. L. Wong, Phys. Fluids B **5** (1993) 4040

[10] G. Y. Fu *et al.*, Phys. Rev. Lett. **75** (1995) 2337

[11] R. Nazikian *et al.*, Phys. Rev. Lett. **78** (1997) 2976

[12] A. Hasegawa, L. Chen, Phys. Rev. Lett. **35** (1975) 370

[13] A. Jaun *et al.*, Plasma Phys. Contr. Fusion **39** (1997) 549

[14] A. Jaun, J. Vaclavik, L. Villard, Phys. Plasmas 4 (1997) 1110

[15] A. Fasoli *et al.*, Phys. Rev. Lett. **75** (1995) 645

[16] A. Jaun, J. Vaclavik, L. Villard, *Global Alfvén Eigenmodes Stability in ITER*, 5th IAEA Tech. Com. on *Alpha Particles in Fusion Research*, 8-11 September 1997, JET

[17] L. L. Lao *et al.*, Nucl. Fusion **30** (1990) 1035

[18] H. Lütjens, A. Bondeson, O. Sauter, Comput. Phys. Commun. **97** (1996) 219

[19] A. Jaun *et al.*, Comput. Phys. Commun. **92** (1995) 153

[20] S. Brunner, J. Vaclavik, Phys. Fluids B **5** (1993) 1695

[21] A. Jaun *et al.*, in proc. 12th Topical Conf. RF power in Plasmas, Savannah (1997), AIP in press

[22] A. Fasoli *et al.*, Phys. Rev. Lett. **76** (1996) 1067

[23] W. W. Heidbrink *et al.*, Phys. Plasmas (1997), accepted